

CHAPTER 4

Giglio Island: intrusive magmatism

DAVID S. WESTERMAN¹, FABRIZIO INNOCENTI² and SERGIO ROCCHI^{2*}

¹ Norwich University, Department of Geology, Northfield, Vermont 05663, USA

² Dipartimento di Scienze della Terra, Università di Pisa, Via S. Maria, 53, Pisa, 56126, Italy

4.1 HISTORICAL PERSPECTIVE

Giglio Island, first populated during the Palaeolithic, was called Aigilion Mikros by the Greeks («Small Land of Goats», while Capraia was Aigilion Mikros, «Great Land of Goats»), and later Igilium by the Romans. In the fifth century, after the fall of the Roman Empire, the Tuscan islands become retreats and refuges for small communities of Christian monks. Dominated by the Republic of Pisa in medieval times, all the islands suffered attacks and robberies by Turkish pirates in the sixteenth century.

4.2 GEOLOGIC SETTING

The northern Tyrrhenian Sea is a region affected by extensional processes behind the eastward migrating compressive regime in the hanging wall of the eastward retreating Apennine slab. After the early Miocene compressive phase, the orogenic system evolved diachronously as the regime of extension migrated from west to east, trailing the retreat of the compressive regime and giving way to the opening of the Tyrrhenian

basin. In this framework, magmas were generated in the mantle and interacted with crust-derived felsic magmas to generate the variety of Tuscan Magmatic Province intrusive and extrusive products. This igneous activity migrated from west (14 Ma) to east (0.2 Ma) in an extensional ensialic back-arc setting as the west-dipping Adriatic plate delaminated and rolled back to the east (Serri *et al.*, 1993). In early Pliocene time, intrusive activity affected the area of Giglio Island. This island, located 20 km off the Tuscan coast of Italy, rises to elevations near 500 m along an axis trending N20W. Greater than 90% of its 20 km² of exposed surface area is underlain by granitic rocks (Fig. 1).

4.3 THE INTRUSIVE UNITS

Two distinct intrusions can be recognised on Giglio Island (Fig 1; Westerman *et al.*, 1993). The older and much larger of the two, the Giglio monzogranite intrusion (GMI), is composed of two facies, the Arenella facies (ARF) and the Pietrabona facies (PBF). Although Rb-Sr geochronological data on Giglio rocks and minerals record the occurrence of minor isotopic disequilibrium, the emplacement age of all the intrusive units

* Corresponding author, E-mail: rocchi@dst.unipi.it

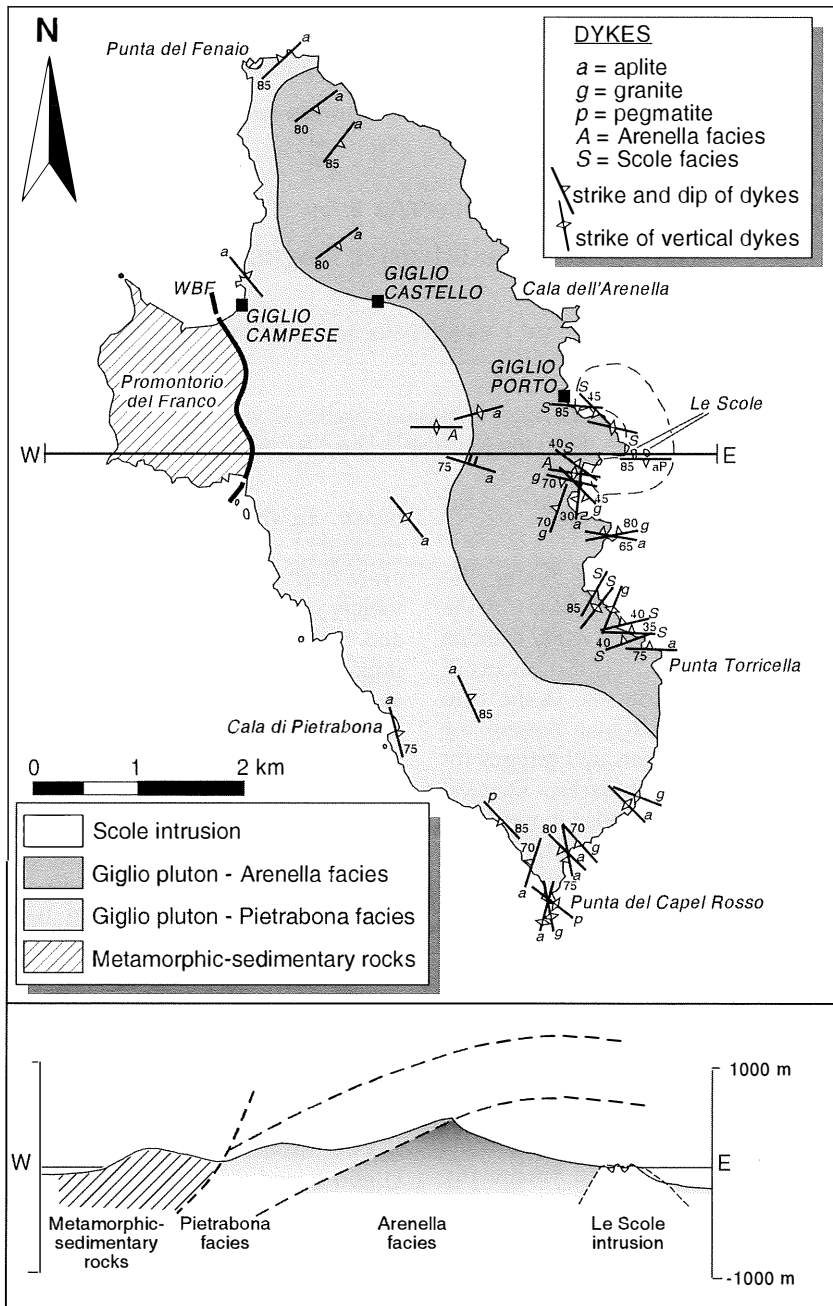


Fig. 1 – Geological map and cross section of Giglio Island. Intrusive units include the Giglio monzogranite intrusion (Arenella Facies and Pietrabona Facies), the Scole monzogranite intrusion (SMI), and dykes of aplite, granite, pegmatite, Arenella Facies and Scole intrusion. Additional symbols are for the Western Border Fault (WBF). Modified after Westerman *et al.* (1993).

can be constrained at ca. 5.0 Ma (Westerman *et al.*, 1993).

4.3.1 Giglio monzogranite Intrusion (GMI)

Arenella facies (ARF). Rocks of the ARF are recognised on the basis of (1) abundant, coarse, cream-coloured K-feldspar megacrysts in a medium-grained, grey matrix, and (2) essentially homogeneous textures with the exception of localised preferred orientation of megacrysts. The megacrysts in these rocks stand out both literally due to their greater resistance to erosion, and visually due to their paler colour. These crystals are typically stubby with lengths (2-3 cm) less than twice their widths, and their positive relief produces a «hobnail» texture on weathered outcrop surfaces. Rarely, and only in restricted areas, megacrysts have lengths more than three times their widths. A count of megacrysts having a long dimension of 1 cm or more is approximately 250 per m², corresponding to approximately 10% by volume. Poorly defined zones of leucogranite occur within the ARF, but except for their lower colour index, these rocks are indistinguishable in the field from the more typical ARF rocks.

ARF is strongly porphyritic with K-feldspar, and the paragenesis is characterised by the association of dominant plagioclase, quartz, K-feldspar and biotite. Megacrysts of K-feldspar contain inclusions of fine-grained plagioclase, biotite and quartz, and locally have graphic overgrowths with quartz and orthoclase. Alteration of K-feldspar to kaolinitic products is common. Plagioclase is generally subhedral with An₄₀ nuclei that change through oscillatory zoning to oligoclase rims. Opaque minerals are generally associated with the biotite. Minor muscovite, iron-rich tourmaline, apatite and zircon are observed. Cordierite, generally transformed to pinite, is common with relicts having $(Fe+Mn)/(Fe+Mn+Mg)=0.44$. Biotite in the GMI are generally weakly zoned with $Fe/(Fe+Mg)=0.52$ in the core and 0.57 in the rims. Scattered Fe-rich garnet broken down to the assemblage muscovite-chlorite-quartz, along with andalusite with reaction coronas

have been observed throughout the intrusion. Sillimanite needles have been identified within quartz grains. Monazite, sphene and pyrite are rare. Secondary minerals associated with deuteric alteration and/or later hydrothermal activity are represented by muscovite flakes forming from feldspars, rutile needles and chlorite after biotite, and epidote, calcite and iron oxide.

Pietrabona facies (PBF). Rocks of the PBF, in contrast to those of the ARF, are characterised by the presence of layering that is locally very pronounced (Fig. 2). This layering is visible due to (1) the preferred orientation of elongated or flattened xenoliths, (2) the preferred orientation of biotite and feldspar crystals as well as mosaic quartz ribbons producing a foliation and, in many instances, a gneissic layering, and (3) differential erosion of light and dark bands due to rhythmic changes in modal proportions, most notably of biotite and cordierite. The more felsic bands stand out in raised relief. At many locations the layers have a strong planar character although gentle undulation of the layering is common over distances of 100 m or less. Gneissic layering with strong, abrupt changes in biotite content on a scale of 10 cm occurs only along the western margin of the granite near the faulted contact with the metamorphic and sedimentary rocks of the Franco Promontory. Platy xenoliths there are oriented parallel to the igneous foliation that dips gently toward the west. The transition zone between PBF and ARF is marked by an abundance of large crystals of K-feldspar (1-3 cm). The contact between the two facies has been modelled at depth as westward dipping (21-54°) on the basis of a geomagnetic survey (Faggioni *et al.*, 1998).

ARF and PBF show some common features. The mineral assemblage for both the ARF and the surrounding non-porphyritic PBF is the same. Also a great variety of metamorphic xenoliths and mafic microgranular enclaves (MME) are ubiquitous in both facies. MME may be as big as 2 m, have finer grain size and similar colour index and mineralogy with respect to the host granite, so that in some

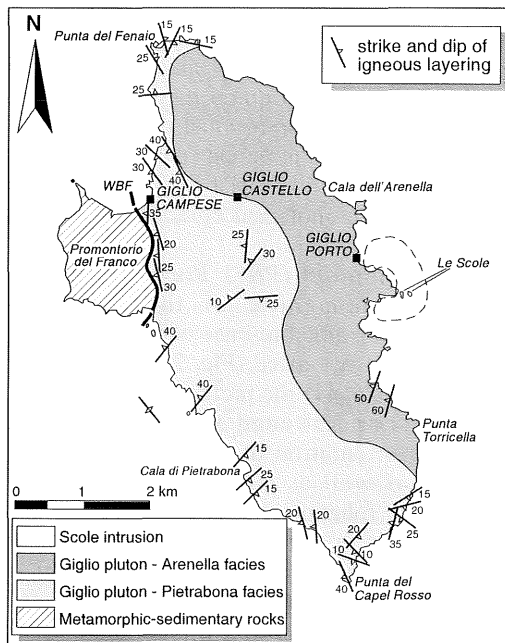


Fig. 2 – Map of igneous layering. Modified after Westerman *et al.* (1993).

instances they are hard to detect. The smallest MME show the greatest variations in colour index. Within the layered zones of PBF, the enclaves commonly have high aspect ratios (around 10), while outside that zone, MME commonly approach spherical shapes with rounded borders. Metamorphic xenoliths with either rounded or angular borders include biotite-rich quartzofeldspathic schists and high-grade schists and gneisses.

4.3.2 Scole monzogranite intrusion (SMI)

The Scole monzogranite intrusion (SMI) (Westerman *et al.*, 1993) crops out in limited extent along the easternmost margin of the island in the area of the Scole islets (Fig. 1). It is distinctly more acidic than the GMI and has exposed intrusive contacts with the ARF. The diagnostic properties of the SMI include (1) a low colour index (CI ca. 7) and distinctive buff-weathering outcrop surfaces, (2) homogeneous and isotropic, weakly-

porphyritic texture with K-feldspar megacrysts, (3) black tourmaline clots, and (4) a notable absence of xenoliths and MME that are so characteristic of the GMI. Sub- to euhedral megacrysts of K-feldspar in these SMI rocks are typically 1-1.5 x 2-3 cm and occur scattered throughout with random orientation. The concentration of megacrysts with a minimum dimension of 1 cm on the outer Scole islet is approximately 100 per m², approximately 60% lower than is characteristic for rocks of the ARF that they intrude. Also characteristic of these rocks of the SMI is the presence of rounded black tourmaline clots with diameters of 2-3 cm and rims or intergrowths of feldspar. Their abundance is generally less than 5 vol%, but local values approach 10%. Such tourmaline clots also occur within the GMI rocks, but in SMI they stand out due to the lower colour index and uniform texture of the host. The matrix of the SMI is fine to medium grained consisting of quartz, two feldspars, biotite, tourmaline, and cordierite.

Contacts of the SMI on the Scole islets, as well as on the east edge of the main island, show a consistent pattern of gentle westerly dips below the ARF. In the inner Scole islet (the western one), an injection from the main SMI body can be traced, via a feeder dyke along a complex path in a well-developed orthogonal joint set, into the overlying ARF where it formed a sill that pinches out along a sub-horizontal joint. A similar geometric relationship between rocks of the same two units is exposed along the shore of the main island 300 m west of the Scole islets.

4.3.3 Dykes

Numerous felsic dykes of varying composition cut the GMI (Fig. 1). They are represented primarily by (1) granitic dykes, some of which are garnetiferous with pink crystals (0.1 mm) and distinctly porphyritic with megacrysts primarily of quartz, (2) tourmaline-rich aplite dykes that are often zoned and locally associated with pegmatitic veins, and (3) granitic dykes along the eastern shoreline between Giglio Porto and Punta

Torricella with field characteristics typical of the SMI as described above. Within the SMI, only very minor aplite dykes with associated pegmatite are present.

4.3.4 Country rocks

Intrusive contact relationships between the granites and the surrounding country rock are preserved and exposed only at Punta del Fenaio at the north end of the island (Westerman *et al.*, 1993). There, roof pendants of strongly foliated and hornfelsed argillaceous metasediments dip gently to the north with consistent orientations in two areas covering a total of approximately 1,200 m². Exposed intrusive contacts sharply truncate the gently dipping country rock foliation. Foundered blocks of the country rock occur near these contacts.

On the Promontorio del Franco (Fig. 1), an assemblage of Mesozoic metamorphic and sedimentary rocks is in fault contact with the intrusive rocks along the Western Border Fault (WBF; Westerman *et al.*, 1993). This assemblage is composed of a stack of tectonometamorphic units (Rossetti *et al.*, 1998, and references therein), including (1) Triassic continental metaclastic and metapelitic rocks (Verrucano), (2) a tectonic mélange of metapelites and calcschists (Verrucano) and lenses of metabasic Ligurian ophiolitic rocks, and (3) upper Triassic dolomites and limestones. These units experienced high pressure metamorphism during the Neogene (Capponi *et al.*, 1997; Rossetti *et al.*, 1999, and references therein), and represent a keystone for the reconstruction of the tectonic evolution of the Apennine-Alpine belt.

Sedimentary rocks close to the WBF generally show no evidence of thermal metamorphism, suggesting that subsequent to the emplacement of the monzogranitic rocks of Giglio at 5 Ma, there has been a component of vertical movement on the WBF that is at least equal the thickness of the contact aureole surrounding the plutonic rocks (Rossetti *et al.*, 1998; Westerman *et al.*, 1993). A report of rare, discontinuous levels of thermally metamorphosed rocks along the contact

suggests the possibility that the WBF may have reworked an original intrusive contact (Capponi *et al.*, 1997).

4.4 GEOCHEMISTRY AND PETROGENESIS

On the whole, the main intrusive mass (the GMI with its two facies ARF and PBF) shows relatively little mineralogical or chemical variation (Table 1); all these rock compositions plot within the monzogranite field of normative Q' vs. ANOR (Fig. 3). Samples from the younger SMI plot astride the monzogranite-syenogranite fields. Silica content of all the intrusive rocks ranges between 67 and 73 wt% while the alkali content is relatively constant between 7-8 wt% (Fig. 4, 5). Alumina saturation index (ASI) is consistently greater than 1.1, stressing the peraluminous character of these rocks. Samples of SMI are significantly more peraluminous (ASI = 1.28) than are those of the main intrusion (average value of ASI = 1.14±0.03). Leucocratic masses occurring locally within the GMI display compositions within both the monzo- and syenogranite fields. Dykes cutting the main intrusions vary considerably in composition from more basic than the main mass to more felsic, with the most felsic represented by the late stage, tourmaline-bearing aplites with or without associated pegmatite. Samples of the leucocratic facies are depleted in Sr, Ba, La and Zr; these trace elements distributions can be interpreted as resulting of crystal fractionation processes involving mainly plagioclase and, subordinately, accessory minerals like monazite, apatite, tourmaline and zircon. The SMI samples exhibit lower contents of Y and Ba, and (to a less extent) of Zr, Nb and La with respect to the main intrusion, while Rb and Sr abundances are in the same range.

The main intrusion (GMI) exhibits initial Sr isotopic compositions ranging from 0.7163 to 0.7176 and ¹⁴³Nd/¹⁴⁴Nd are in the range 0.51217-0.51222. In contrast, the rock samples from the SMI are characterised by higher (0.7195 – 0.7203) Sr and lower (0.51205 –

TABLE 1
Chemical analyses of intrusive rocks from the Giglio Island (after Westerman et al., 1993)

unit	GMI - Arenella facies					GMI - Pietrabona facies					SMI - Le Scole leucofacies					dyke	MME (mafic enclaves)			
Sample	G1	G8	G9a	G10	G13	G55a	G56	G16	G24	G61	G62	G18	G31	G50	G3	G9b	G55b	G59	G2	G12b
<i>Major elements (wt%)</i>																				
SiO ₂	67.71	67.46	68.04	67.66	68.34	87.79	66.96	67.15	67.22	68.09	67.85	66.59	70.67	69.81	71.63	73.18	66.60	67.60	66.47	64.90
TiO ₂	0.71	0.75	0.65	0.62	0.66	0.62	0.66	0.61	0.66	0.60	0.62	0.65	0.37	0.56	0.43	0.27	0.76	0.82	0.91	0.78
Al ₂ O ₃	15.31	15.50	15.43	15.47	15.26	15.30	15.68	15.96	15.75	15.64	15.51	16.07	15.97	15.30	14.48	14.07	15.41	15.49	15.11	16.52
Fe ₂ O ₃	1.17	1.07	0.99	1.13	1.07	1.28	1.20	1.17	1.14	1.07	1.05	1.15	0.96	1.36	0.78	0.56	1.14	1.12	1.35	1.23
FeO	2.68	2.75	2.77	2.71	2.50	2.48	2.83	2.53	2.66	2.49	2.65	2.63	0.95	1.91	1.84	1.13	2.87	2.47	3.78	3.47
MnO	0.06	0.04	0.06	0.06	0.05	0.06	0.06	0.06	0.05	0.06	0.06	0.07	0.02	0.05	0.05	0.04	0.06	0.05	0.08	0.10
MgO	1.21	1.20	1.15	1.20	1.20	1.22	1.39	1.23	1.36	1.26	1.26	1.50	0.71	0.86	0.79	0.51	1.31	0.82	1.88	1.72
CaO	2.06	2.19	1.95	2.07	2.11	2.19	1.93	1.96	2.08	1.85	1.90	2.32	1.37	1.70	1.57	1.20	2.38	2.00	1.90	2.85
Na ₂ O	2.78	2.75	2.86	2.90	2.63	2.64	2.93	2.76	2.86	2.93	2.97	2.78	2.92	2.25	2.60	2.56	2.96	3.40	2.70	3.29
K ₂ O	5.08	4.91	4.67	4.82	5.00	4.97	4.75	5.01	4.87	4.77	4.82	4.63	4.80	4.79	4.97	5.56	4.62	5.28	4.20	3.08
P ₂ O ₅	0.23	0.22	0.25	0.22	0.25	0.25	0.23	0.27	0.22	0.23	0.22	0.21	0.13	0.20	0.17	0.13	0.26	0.20	0.18	0.27
LOI	1.00	1.16	1.16	1.14	0.73	1.20	1.14	1.29	1.14	1.00	1.06	1.20	1.13	1.21	0.69	0.79	1.43	0.75	1.44	1.79
<i>Trace elements (ppm)</i>																				
Rb	314	281	326	283	299	273	262	280	276	303	314	287	309	270	278	315	267	309	307	252
Sr	137	160	112	135	156	156	179	150	166	141	147	151	161	143	107	96	144	166	164	90
Y	33	32	32	30	32	32	30	33	33	32	33	34	24	27	32	29	35	40	26	33
Zr	214	219	213	198	210	208	208	226	217	206	199	215	146	202	157	103	257	388	245	223
Nb	17	16	18	16	15	12	15	16	15	15	15	16	10	15	13	10	16	19	17	20
Ba	441	434	428	414	419	504	469	441	477	455	426	430	341	403	320	236	424	819	928	262
La	38	35	31	38	34	34	37	36	37	33	37	34	27	31	30	18	45	58	32	38
Ce	71	75	65	72	72	71	73	77	73	67	75	66	48	57	65	32	92	109	59	29

Analytical techniques: MgO, Na₂O and K₂O determined by AAS; FeO by titration ; LOI by gravimetry at 1000°C, assuming complete oxidation of Fe²⁺. Other major elements and trace elements determined by XRF on powder pellets. For trace elements the precision is estimated better than 5% for abundances greater than 10 ppm.

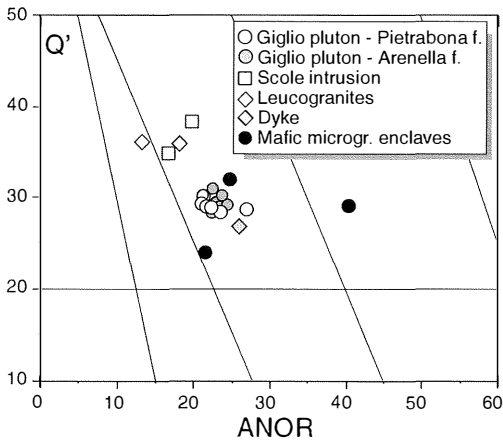


Fig. 3 – Normative Q' vs. ANOR classification diagram (Streckeisen and Le Maitre, 1979). Modified after Westerman *et al.* (1993).

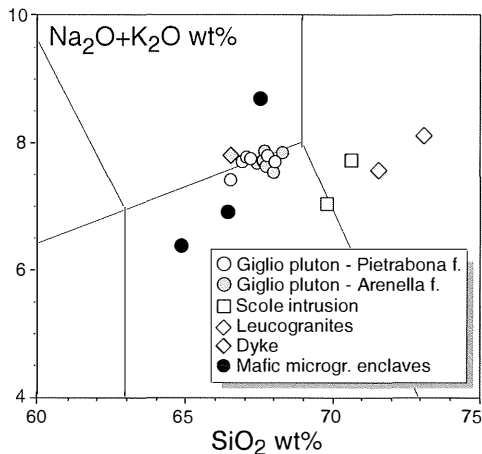


Fig. 4 – TAS diagram (Le Bas *et al.*, 1986). Modified after Westerman *et al.* (1993).

0.51207) Nd isotopic compositions, among the highest and lowest, respectively, from the whole Tuscan Magmatic Province (see Part III, Chapt. 2, Fig. 12). These isotopic ratios, coupled with the occurrence of distinctive peraluminous minerals, point out the prominent role of partial melting of metasedimentary crustal material in the genesis of the intrusive rocks of Giglio (Westerman *et al.*, 1993).

Additionally, different crustal sources have to be inferred for GMI and SMI.

MME represent enclaves of mafic magma included in the primary GMI magmas as liquid or in a crystal-mush state (Poli, 1992). The hybrid mineralogy and the isotopic composition of phases separated from some of the Giglio MME indicate that they experienced different degrees of equilibration with the host magma, leading in some cases to a complete homogenisation ($^{87}\text{Sr}/^{86}\text{Sr} = 0.7128\text{-}0.7172$). The occurrence of this kind of enclaves at Giglio support the hypothesis that mixing has played a pivotal role in the genesis of the TMP granitoids (Poli, 1992; Innocenti *et al.*, 1997; Dini *et al.*, 2002; Serri *et al.*, 1993). In this frame, the lack of Sr-isotope homogeneity for GMI could be ascribed to mixing processes rather than to source heterogeneity. The mixing end-members are difficult to detect, owing to the likely absence of melt that totally escaped mixing processes. Thus, the isotopic compositions of some metamorphic xenoliths and mafic enclaves can only point the direction to the actual composition of the felsic and mafic end-members, respectively.

Additionally, the younger SMI show isotopic compositions that cannot be explained by the same model (or the same end-members) as GMI. Indeed, GMI and SMI formed from two geologically and geochemically distinct magmatic injections of slightly different age. These observations are constraints for the general hybridisation model for TMP discussed in the «Geochemistry and Petrogenesis» section of Part III, Chapt. 2 (Dini *et al.*, 2002).

4.5 EMPLACEMENT OF MAGMA

Although the main intrusion is not visible in all its planar extension due to the presence of the sea, the shape of the body in map view is interpreted to be elliptical or circular. The main intrusion (GMI) is structurally and compositionally zoned with continuous variation between the different facies. The outer part is foliated and displays a flattening fabric that constitutes a petrographic evidence

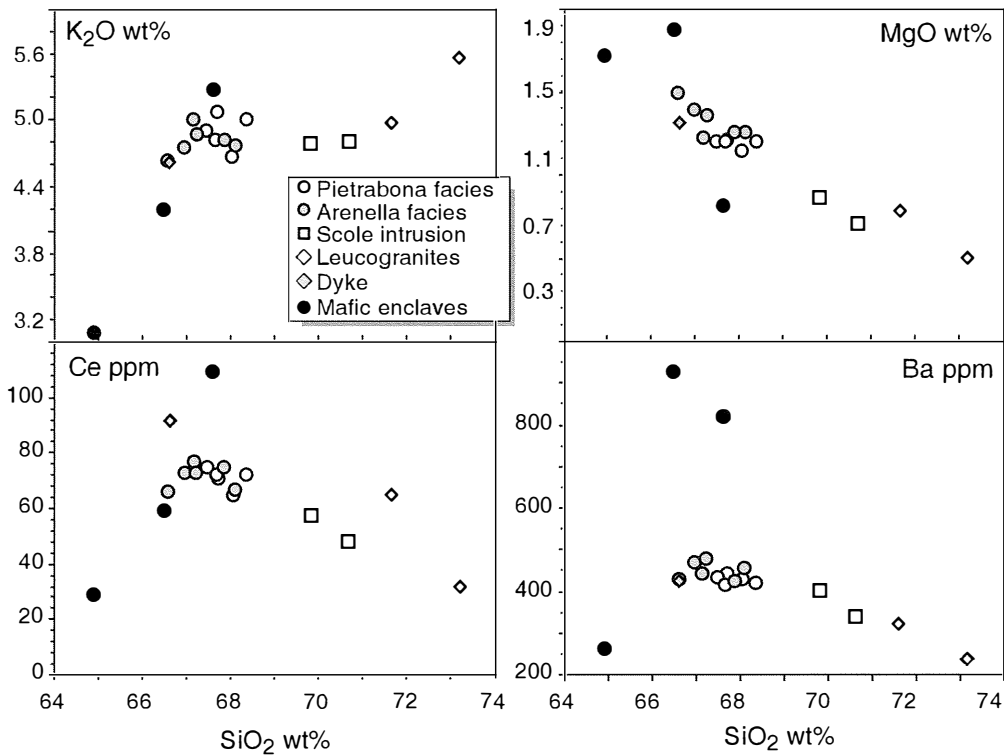


Fig. 5 – Selected variation diagrams for Giglio intrusive rocks.

of strain experienced by the intrusive body during the emplacement, possibly due to ballooning (Faggioni *et al.*, 1998) or to magma emplacement linked to an east-dipping extensional shear-zone (Rossetti *et al.*, 1999). The inner zone is strongly porphyritic and non-foliated, and contains scattered areas of more leucocratic rocks of syeno-monzogranitic composition. Following sufficient solidification to allow the development of joints in the Giglio monzogranite intrusion, a distinctly different magma derived from a separate source area, was emplaced to form the Scole monzogranite intrusion (SMI).

4.6 CONCLUSIONS

The Tuscan Magmatic Province is located in an extensional area that is considered

structurally equivalent to a back arc basin, but in a continental crust setting. Here, the crust experienced partial melting with mixing of crustal acidic magmas and mantle mafic melts. The formation of a wide region of anatexis and hybridisation may have produced an effective buffer zone, preventing the upwelling and the eruption of the subcrustal melts. Whatever the cause, primary basic products are absent within the ellipsoidal region (150x300 km) centred on the Island of Giglio, while they are more common at the space-time border of it.

This paper is based on the work of D.S. WESTERMAN, F. INNOCENTI, S. TONARINI and G. FERRARA titled *The Pliocene intrusions of the Island of Giglio (Tuscany)*, published in *Memorie della Società Geologica Italiana*, vol. **49**, 345-363, 1993.